Thermal shock behaviour of unidirectional, 0°/90°, and 2-D woven fibre-reinforced CVI SiC matrix composites

H. WANG, R. N. SINGH
Department of Materials Science and Engineering, University of Cincinnati, P.O. Box 210012, Cincinnati, OH 45221-0012 USA

R. A. LOWDEN
Metals and Ceramics Division, Oak Ridge National Laboratory, Oak Ridge, TN 37831-6063 USA

The thermal shock behaviour of Nicalon™ fibre-reinforced chemical vapour infiltrated SiC matrix composites with three different types of fibre architecture, unidirectional, 0°/90°, and 2-D woven, has been studied using the water quench technique. Thermal shock induced damage was characterized by the destructive four-point flexure technique and the nondestructive technique of Young's modulus measurement by the dynamic resonance method. It was shown that the unidirectional and 0°/90° composites did not possess satisfactory mechanical properties or resistance to thermal shock because these fibre architectures prevented the composites from attaining high density during infiltration. Excess carbon coating was also found in the unidirectional and 0°/90° composites. Oxidation of this carbon coating contributed to the property degradation at high quench temperature difference. By contrast, the composite with 2-D woven fibre architecture created using the 0°/30°/60° cloth lay-up showed superior mechanical properties and thermal shock resistance. The nondestructive technique of Young's modulus measurement by the dynamic resonance method was successfully used in detecting the thermal shock damage.

1. Introduction

In a previous paper by the authors [1] the effects of fibre materials and matrix processing techniques on the thermal shock behaviour of continuous fibre-reinforced ceramic composites (CFCCs) were demonstrated. It was proposed that different stress states would be generated in composites subjected to thermal transients because of the difference in the coefficients of thermal expansion between fibres and matrices, leading to different damage evolution processes in the fibre-reinforced composites.

In comparison to monolithic ceramics, continuous fibre-reinforced ceramic composites have a superior resistance to thermal shock, but they display a much more complex behaviour under thermal transient conditions [1–3]. In addition to the influence of the fibre material and matrix processing techniques, many other factors, including the types of fibre architecture, can affect the thermal shock behaviour of fibre-reinforced composites. Several types of fibre architectures have been used for reinforcing ceramic composites, including unidirectional, 0°/90°, two-dimensional (2-D) weaves, and three dimensional (3-D) hybrid forms [4]. Extensive studies, both experimental and theoretical, have been conducted on the performance of unidirectional composites [5–14], their anisotropic character makes them less suitable for real applications than for modelling. Composites with 0°/90°, fibre architecture are developed to alleviate some of the problems associated with uniaxial composites, but only limited studies regarding their properties have been performed [15, 16]. Recently, composites made of two-dimensional (2-D) woven fibres have attracted a considerable amount of interest because of their superior properties as well as ease in processing by CVI (chemical vapour infiltration) over the unidirectional and 0°/90° fibre-reinforced composites. The properties of various 2-D woven fibre-reinforced ceramic composites have been studied at both room and elevated temperatures [17–29].

However, no systematic study of the effects of fibre architecture on the behaviour of fibre-reinforced ceramic matrix composites under transient thermal conditions has been reported. Fibre-reinforced ceramic composites are primarily designed for use in high temperature applications where they are often subjected to transient thermal environments or thermal shock, which can cause fracture, property degradation, and accelerated chemical corrosion of the composites. Thus, it is essential to understand the

0022–2461

behaviour of fibre-reinforced composites under thermal transients and the associated damage mechanisms, so that this knowledge can be used to guide the selection of materials, processing techniques, and component design.

This paper reports on the thermal shock behaviour of Nicalon™ fibre-reinforced SiC matrix composites with unidirectional, 0°/90°, and 2-D woven fibre architectures and fabricated by CVI. The objectives of this study were to examine the influence of fibre architecture on the thermal shock behaviour of composites and to investigate the thermal shock damage mechanisms.

2. Experimental procedures

The composites tested in the present study had a chemical vapour infiltrated (CVI) SiC matrix and Nicalon™ fibre reinforcement of three different architectures: unidirectional, 0°/90°, and 2-D weave, herein after referred to as the unidirectional, 0°/90°, and 2-D composites, respectively. They were supplied by Oak Ridge National Laboratory.

Composites with different fibre architectures were created using different fibre preforms. In the unidirectional composite, fibres were aligned unidirectionally throughout the preform. In the 0°/90° composite, fibres were aligned in orthogonal directions in alternate layers. 2-D plain woven cloths were used for the 2-D woven composites. The cloths were rotated $\pm 30^\circ$ with each other in the preform, as this arrangement yielded a large permeability for the vapour infiltration. The fibre volume fraction was around 40% in all the composites. The preforms were coated with an interfacial carbon layer via the deposition from a mixture of argon and propylene at 1375 °C and 3.3 kPa. The SiC matrix was produced by forced flow, thermal gradient infiltration of methyltrichlorosilane (MTS), CH_3SiCl_3, and hydrogen using a hot-surface temperature of 1200 °C. The final composite densities were about 2.0, 2.1 and 2.6 g cm^{-3} for the unidirectional, 0/90, and 2-D composites, respectively.

Specimens for the thermal shock study were cut from as-received plates or billets. The specimen dimensions were $3 \times 5 \times 50$ mm for the unidirectional and 0°/90° composites, and $3 \times 6 \times 50$ mm for the 2-D composite. The tensile surfaces of the specimens were parallel to the fibre and 0° fibre, respectively, in the unidirectional and 0°/90° composites, and parallel to the fibre cloths in the 2-D composite.

A water quench technique was employed to study the thermal shock behaviour of these fibre-reinforced composites. Details of the test procedure have been given elsewhere [1, 3]. Damage to the composites induced by the thermal shock was characterized using destructive and nondestructive techniques. The destructive technique involved subjecting the composites to a 4-point flexure test and recording the load–displacement data from which the change in the composite's ultimate strength, matrix cracking stress, work of fracture, and modulus of elasticity were determined. The flexure tests were conducted using a universal testing machine (Model 4206, Instron Corp., Canton, MA) with the loading and supporting spans of 20 and 40 mm, respectively. The crosshead speed was 0.5 mm min^{-1}. Due to the limitation on sample quantity, most of the data were collected with one specimen for each data point.

The nondestructive evaluation (NDE) technique studied in the present research consisted of measuring the Young's modulus before and after the water quench using a dynamic mechanical resonance technique (GrindoSonic MK5, J. W. Lemmens Co., St. Louis, MO). Details of this technique have been reported previously [1, 3]. Bar-shaped specimens used for the strength test were also used for the Young's modulus measurement. The effect of thermal shock on the Young's modulus was examined as a function of quench temperature difference.

Scanning electron microscopy (SEM) (JSM-T220A, Jeol-Technics Co., Ltd, Tokyo, Japan) was employed to study the microstructures of the as-received and thermally shocked composite samples. The surfaces of some specimens were polished to a 1 μm finish using diamond pastes before the thermal shock to facilitate the microstructural examination.

3. Results

3.1. Failure modes of the three composites

The three as-received composites exhibited different failure modes in the flexure test, as is shown in Fig. 1. The unidirectional and 0°/90° composites failed by delamination and the 2-D composites by tensile fracture. No change in the failure modes because of the thermal shock was observed. Fig. 2 shows the stress–displacement curves for the three composites in their as-received state ($\Delta T = 0$ °C). The unidirectional and 0°/90° composites failed by interlaminar shear (delamination) fracture, and each sharp decrease in the stress–displacement curve (Fig. 2) corresponds to a shear failure. After unloading, the specimens almost regained their original shapes, as is shown in Fig. 1. On the other hand, the 2-D composite specimens fractured through the fibre planes, no interlaminar shear failure was observed, and the fracture involved

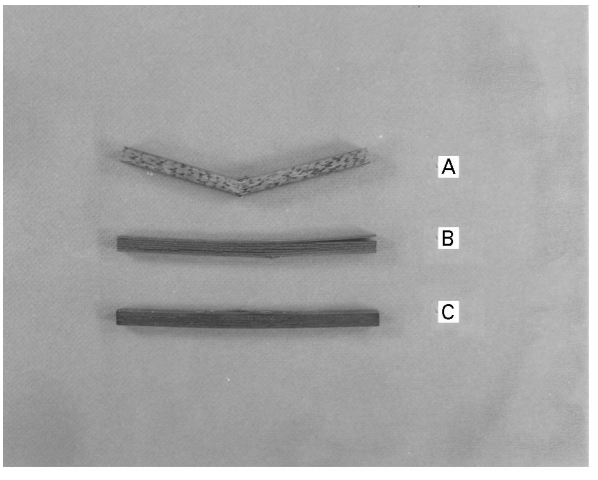

Figure 1 Failed specimens after the flexure tests of (A) 2-D, (B) unidirectional, and (C) 0°/90° composites.

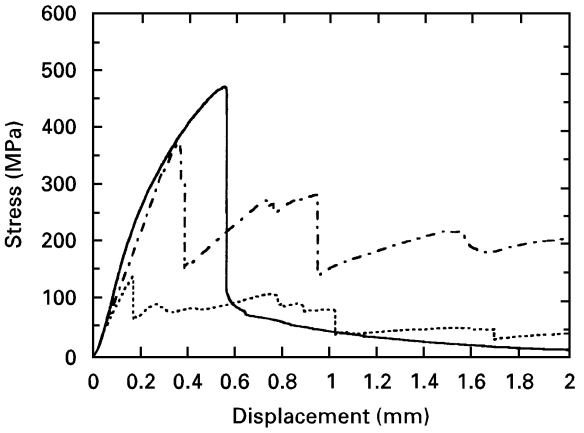

Figure 2 Stress-displacement curves of Nicalon™ fibre/CVI SiC composites with: (– - –) unidirectional, (···) 0°/90° and (—) 2-D fibre architectures (unquenched).

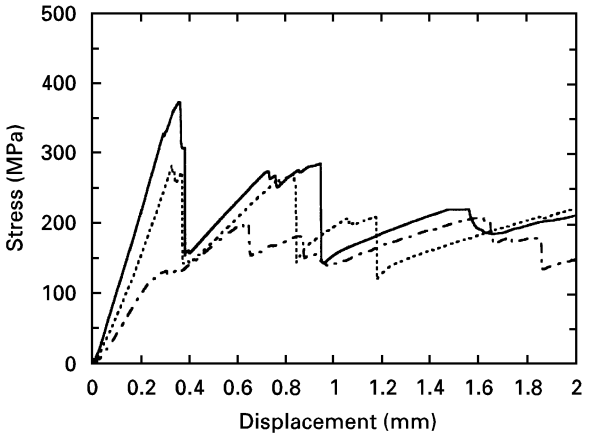

Figure 3 Effect of the quench temperature difference on the stress–displacement curves of the unidirectional Nicalon™ fibre/CVI SiC composite. The investigated temperatures were: (—) $\Delta T = 0\,^{\circ}C$, (···) $\Delta T = 350\,^{\circ}C$ and (— - —) $\Delta T = 1000\,^{\circ}C$.

fibre breakage. It is noted in Fig. 2 that the 2-D composite has the highest ultimate strength and the 0°/90° the lowest. Also, the 2-D composite exhibits a significant non-linear behaviour prior to fracture, which is different from the unidirectional and 0°/90° composites. In the following, the effects of thermal shock on the stress–displacement behaviour and various properties of the three composites are discussed.

3.2. Unidirectional Nicalon™ fibre/CVI SiC composite

The effect of an increasing quench temperature difference (ΔT) on the stress–displacement behaviour of the unidirectional composite is shown in Fig. 3. It is seen that an increasing severity of the thermal shock affects most of the properties that are determined from the stress–displacement curve, including the ultimate strength (σ_u), the matrix cracking stress (σ_{mc}), the work of fracture (WOF), and the Young's modulus. Fig. 4 plots the ultimate and matrix cracking strengths of the composite as a function of ΔT. It is seen that the σ_{mc} and σ_u follow essentially the same trend with increasing ΔT. There exists a critical

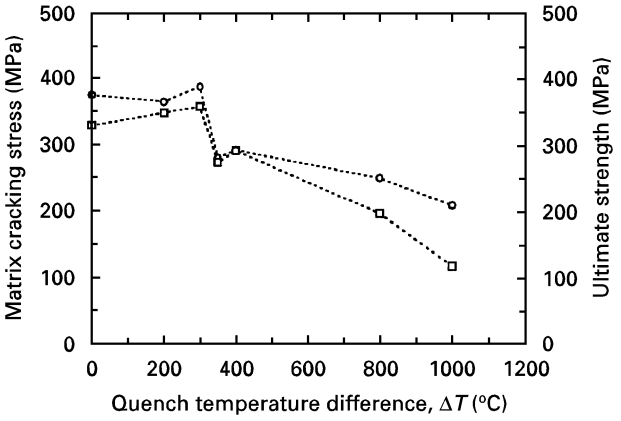

Figure 4 Effects of the quench temperature difference on the: (○) ultimate (σ_u) and (□) matrix cracking strengths (σ_{mc}) of the unidirectional Nicalon™ fibre/CVI SiC composite.

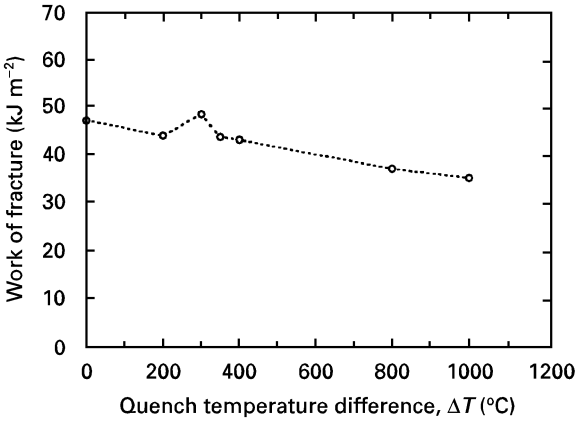

Figure 5 Effect of the quench temperature difference on the work-of-fracture of the unidirectional Nicalon™ fibre/CVI SiC composite.

quench temperature difference, ΔT_c, at which both the σ_{mc} and σ_u show a significant decrease. Above this ΔT_c, a gradual decrease is seen for the ultimate strength, and a steeper drop is exhibited by the matrix cracking stress up to $\Delta T = 1000\,^{\circ}C$. The effect of an increasing quench temperature difference on the work of fracture is shown in Fig. 5. It is seen that the WOF of the unidirectional composite only slightly decreases with an increasing ΔT up to $\Delta T = 1000\,^{\circ}C$, and no significant drop in the WOF is seen at the ΔT_c exhibited by the ultimate strength and matrix cracking stress.

3.3. 0°/90° Nicalon™ fibre/CVI SiC composite

Fig. 6 shows the stress–displacement curves of the 0°/90° composite subjected to different quench temperature differences. Similar to the unidirectional composite, the matrix cracking stress, ultimate strength, work of fracture, and Young's modulus are all affected by the thermal shock. Fig. 7 illustrates the change in the ultimate and matrix cracking strengths brought about by the thermal shock. Similar to the unidirectional composite, the ultimate and matrix cracking strengths show the same ΔT_c of 350 °C. Also

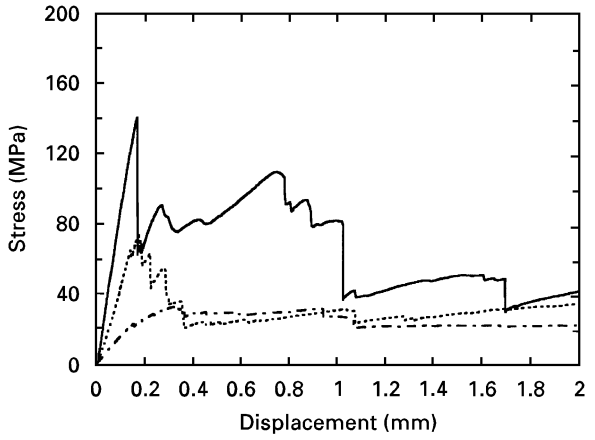

Figure 6 Effect of the quench temperature difference on the stress–displacement curves of the 0°/90° Nicalon™ fibre/CVI SiC composite. The investigated ΔT values were: (—) 0 °C, (···) 400 °C and (– – –) 1000 °C.

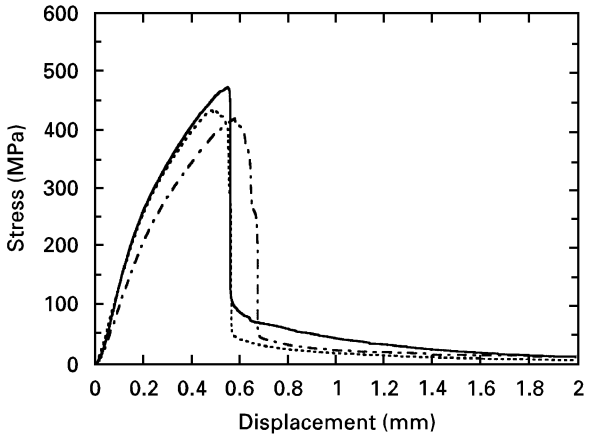

Figure 9 Effect of the quench temperature difference on the stress–displacement curves of the 2-D Nicalon™ fibre/CVI SiC composite. The investigated ΔT values were: (—) 0 °C, (···) 800 °C and (– – –) 1000 °C.

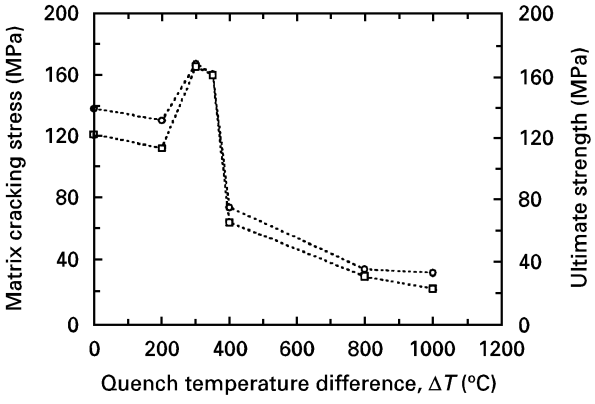

Figure 7 Effects of the quench temperature difference on the: (○) ultimate strength and (□) matrix cracking stress of the 0°/90° Nicalon™ fibre/CVI SiC composite.

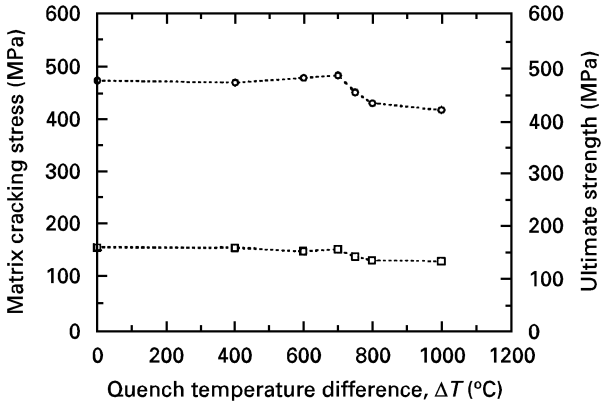

Figure 10 Effects of the quench temperature difference on the: (○) ultimate strength and (□) matrix cracking stress of the 2-D Nicalon™ fibre/CVI SiC composite.

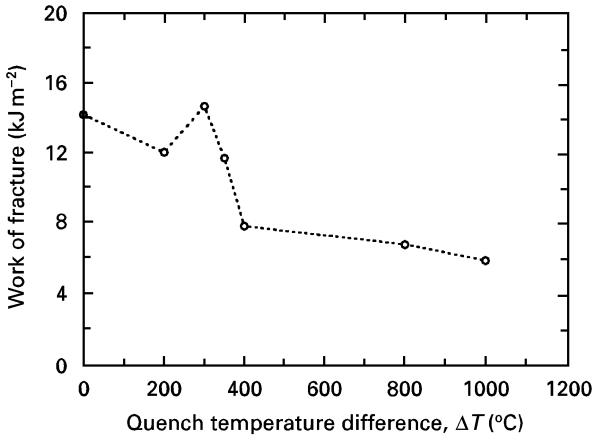

Figure 8 Effect of the quench temperature difference on the work-of-fracture of the 0°/90° Nicalon™ fibre/CVI SiC composite.

noted is a fairly significant increase in both the σ_{mc} and σ_u at $\Delta T = 300\,^{\circ}C$, the exact cause for this increase is as yet unknown. A possibility could be variations in properties from sample to sample. Above ΔT_c, σ_{mc} and σ_u continue to decrease with an increasing ΔT up to $\Delta T = 1000\,^{\circ}C$. A difference from the unidirectional composite behaviour is the observation that the σ_{mc} and σ_u of the 0°/90° composite are close to each other up to the maximum ΔT of 1000 °C. The work of fracture versus quench temperature difference is plotted in Fig. 8. The WOF seems to have a steep decrease at ΔT values between 300–400 °C, above which it decreases only slightly up to $\Delta T = 1000\,^{\circ}C$. Hence, at ΔT values between 300–400 °C, most of the composite properties show a sudden decrease because of the thermal shock damage.

3.4. 2-D woven Nicalon™ fibre/CVI SiC composite

The stress–displacement curves of the 2-D composite subjected to different quench temperature differences are shown in Fig. 9. The slope of the stress–displacement curve, which is a measure of the Young's modulus, only decreased above a ΔT value of 800 °C. The effect of thermal shock on the matrix cracking and ultimate strengths is shown in Fig. 10. It can be seen that the 2-D composite posseses a superior resistance to thermal shock over the unidirectional and 0°/90° composites. The ultimate strength of the 2-D composite is not significantly reduced even at

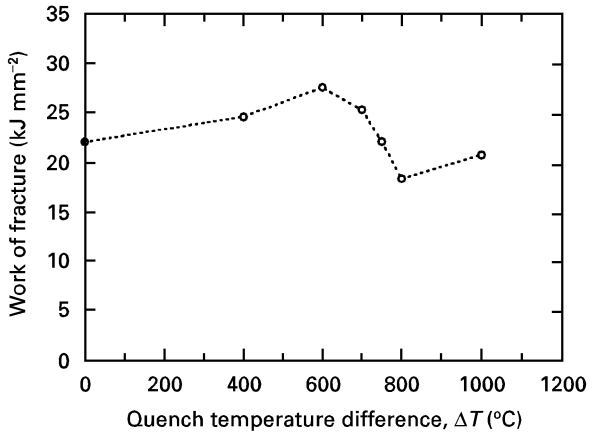

Figure 11 Effect of the quench temperature difference on the work-of-fracture of the 2-D Nicalon™ fibre/CVI SiC composite.

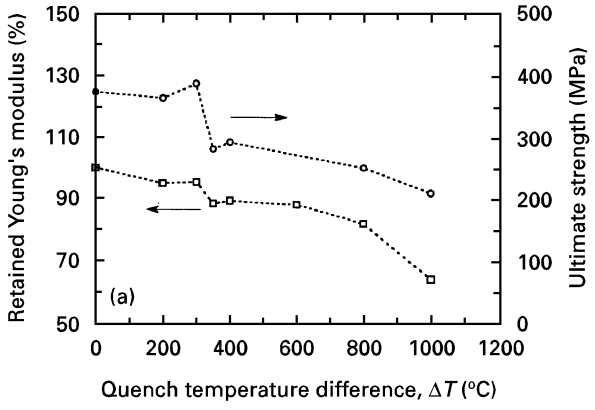

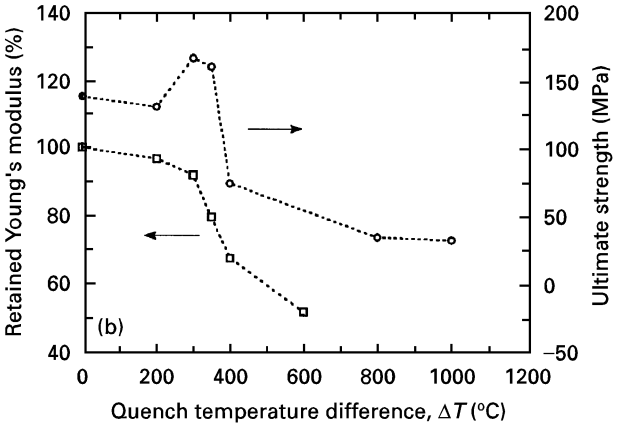

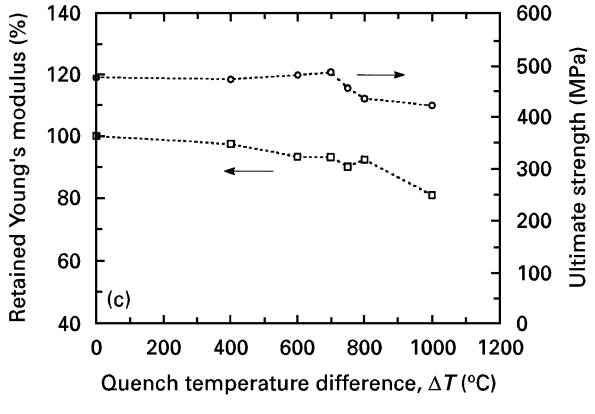

$\Delta T = 1000\,^{\circ}\mathrm{C}$, and the ultimate strength is significantly higher than the matrix cracking strength. The σ_{mc} and σ_u are not degraded up to $\Delta T = 700\,^{\circ}\mathrm{C}$, at which point both properties start to show a slight decrease until $\Delta T = 800\,^{\circ}\mathrm{C}$. Above $\Delta T = 800\,^{\circ}\mathrm{C}$, however, the decrease in σ_{mc} and σ_u seems to have slowed down to the maximum tested ΔT of 1000 °C. The decrease in both the ultimate and matrix cracking strengths is rather small for this composite. At $\Delta T = 700\,^{\circ}\mathrm{C}$, the work of fracture also starts to decrease, as is shown in Fig. 11, but no further decrease is seen between $\Delta T = 800$–$1000\,^{\circ}\mathrm{C}$.

3.5. Non-destructive evaluation

A change in the Young's moduli of the undirectional, 0°/90° and 2-D composites as measured by the non-destructive mechanical resonant technique as a function of the quench temperature difference is shown in Fig. 12 (a–c), respectively. Also plotted for comparison is the change in the ultimate strength determined by the destructive flexure test. For the 0°/90° composite, specimens quenched at $\Delta T > 600\,^{\circ}\mathrm{C}$ delaminated in the water bath because of the thermal stresses, which made the measurement of the Young's modulus impossible. It is seen that, similar to the change in the retained ultimate and matrix cracking strengths, the Young's moduli of the composites change with increasing quench temperature difference. The critical ΔT for the decrease in the Young's moduli measured by the NDE technique coincides with that determined by the destructive flexure test for the unidirectional composite. However for the 0°/90° and 2-D composites, the onset quench temperature differences for the decrease in the Young's modulus seem to be lower than that for the decrease in strength, which indicates that the damage to the composites may have occurred before it could be sensed by the destructive method of strength measurement, i.e., the NDE technique may be more sensitive in detecting thermal shock damage.

4. Discussion

4.1. Effects of fibre architecture

The above results show that the 2-D composite exhibits superior thermal shock behaviour over the unidirectional and 0°/90° composites. The critical quench temperature difference for the decrease in the matrix cracking and ultimate strengths of the 2-D composite is higher than those of the unidirectional and 0°/90° composites, and at the maximum ΔT of 1000 °C, the 2-D composite still possess a larger portion of its original properties.

Contrary to expectation, the unidirectional composite showed a lower ultimate strength in flexure than the 2-D composite. Normally, if the ultimate strength of a fibre-reinforced composite is determined

Figure 12 Effect of the quench temperature difference on the Young's moduli of (a) unidirectional, (b) 0°/90° and (c) 2-D composites measured by the NDE technique. Also shown are the changes in the ultimate strengths.

by the load carrying capacity of the crack-bridging fibres parallel to the tensile direction, then the ultimate strength should be directly proportional to the fraction of fibres aligned with the tensile direction in a flexure test [6, 7]. In a unidirectional composite, all the fibres are aligned with the tensile direction, while in a 2-D composite only a fraction of the fibres are under tension. Therefore, the unidirectional composite is expected to have a higher ultimate strength. The reason for the lower ultimate strength of the unidirectional composite tested in the present study is related to the difference between the failure modes of the unidirectional and the 2-D composites. The ultimate strength of the 2-D composites was controlled by the load-carrying capacity of the fibres because the fracture occurred through the fibre planes. The unidirectional composite, on the other hand, failed by interlaminar shear, and the fracture involved little or no fibre breakage, i.e., the ultimate strength thus measured in our flexure test is the interlaminar shear strength of the matrix. Consequently, the thermal shock performance of the unidirectional composite evaluated by the flexure test is controlled by the properties of the matrix.

Since the unidirectional and 0°/90° composites failed by interlaminar shear, the shear strength of the matrix can be estimated from the ultimate strength measured in the present study. In a flexure test, the specimen experiences the maximum shear stress, τ_{max}, in the midplane of the specimen, while the outer surface of the specimen sees the maximum tensile stress, σ_{max}. Based on the elastic beam theory, the maximum shear and the tensile stresses are calculated as [30].

$$\tau_{max} = \frac{3P}{4bh} \quad (1)$$

$$\sigma_{max} = \frac{3P(L-l)}{2bh^2} \quad (2)$$

where P is the applied load, b and h are the width and thickness of the specimen, and L and l are the outer and inner loading spans, respectively. The ratio of the maximum shear to tensile stresses applied to a specimen is controlled by the specimen dimension and test fixture:

$$\frac{\tau_{max}}{\sigma_{max}} = \frac{h}{2(L-l)} \quad (3)$$

Hence, for the present study, the shear strengths of the unidirectional and 0°/90° composites were about three fortieths of the measured ultimate strengths. For example, the shear strengths of the unquenched unidirectional and 0°/90° composites are 28.1 and 10.4 MPa, respectively. Since the 2-D composite fractured through the fibre planes before the shear stress could reach the shear strength of the interlaminar matrix, the shear strength of the 2-D composite was higher than the maximum shear stress exerted by the load in the flexure test at fracture, i.e., the shear strength of the unquenched 2-D composite was larger than 35.6 MPa.

A microstructural examination revealed the cause for the difference in the failure modes and hence the shear strength of the matrix between the unidirectional and 0°/90° composites, and the 2-D composite. Fig. 13 (a and b) are SEM micrographs showing the cross-section of the unidirectional and 2-D composites, respectively. It can be seen that in the unidirectional composite, the fibres are surrounded with excessive carbon interfacial material which blocks the infiltration of the SiC matrix and results in a higher porosity (lower density). Therefore, the unidirectional composite cannot have an adequate load transfer between the fibres and matrix, which together with its low effective volume fraction of the matrix material and high porosity leads to a matrix of low strength. By contrast, in the 2-D composite, there is a thin and uniform layer of carbon coating around the fibres, and the matrix is filled with relatively dense CVI SiC, which results in the high shear strength of the matrix.

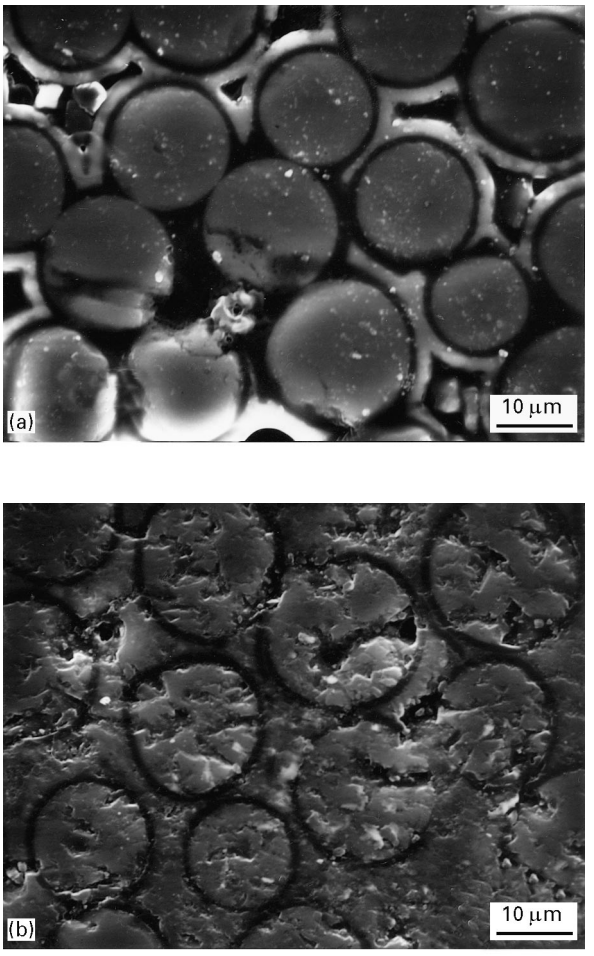

Figure 13 SEM micrographs showing the difference in microstructure between (a) the unidirectional and (b) the 2-D composites (unquenched).

The 0°/90° composite showed an ultimate strength lower than both the 2-D and unidirectional composites. This was not because the 0°/90° composite had about half as many fibres aligned in the tensile direction as in the unidirectional composite, as the fracture did not involve fibres. In the 0°/90° composite, the excessive and non-uniform carbon interfacial coating, similar to the unidirectional composite, exists. In addition, there are many large voids along the 0° and 90° ply boundary. It was observed that the

interlaminar fracture of the 0°/90° composite always occurred along the interply boundary. Therefore, the weaker interply boundary explains the lower ultimate strength of the composite.

The poor microstructure and hence properties of the unidirectional and 0°/90° composites are related to their processing. Stinton *et al.* [27] have shown that because of the anisotropic permeablity of the fibre preforms, it is difficult to obtain a high density for unidirectional fibre-reinforced CVI SiC matrix composites. The permeability along the fibre axial direction is much higher than that in the direction perpendicular to the fibres, hence, reactant gases prefer to penetrate along the length of the fibres and fail to effectively infiltrate into the depth of the preforms. The permeability is improved from the unidirectional to 0°/90° preforms, but a much higher permeability is achieved using the 2-D woven fibre cloths and a 0°/30°/60° lay-up [27]. Since both the carbon fibre coating and the SiC matrix were formed through the CVI process, the anisotropy of the fibre preforms affects the quality of the coating as well as the matrix.

Therefore, the matrix was the "weakest link in the chain" for the unidirectional and 0°/90° composites, which determined their properties, including the thermal shock resistence, of the composites. As stated in our previous paper [1], the decrease in the matrix strength of a composite subjected to thermal shock can be caused by the formation of cracks in the matrix induced by thermal stresses and debonding which changes the interfacial characteristics. The thermal stresses can be generated not only by the temperature gradient between the surface and bulk of the sample as in a monolithic ceramic, but also by the mismatch between the coefficients of thermal expansion of the matrix and fibre. On the other hand, the properties of the 2-D composite are determined by the matrix as well as by the fibre. Its properties, including matrix cracking stress, ultimate strength, work of fracture, and Young's modulus, are affected by such thermal shock damage processes as fibre degradation, debonding, delamination, and matrix cracking [1].

4.2. Effects of oxidation

In the microstructural examination, it was also observed that the carbon coating could be removed by oxidation since in the thermal shock experiment, the specimens were held at high temperatures for about 15 min before being dropped into the water bath. Fig. 14 shows a SEM micrograph of a unidirectional composite specimen subjected to a thermal shock at $\Delta T = 1000\,^{\circ}\mathrm{C}$. The carbon coating material disappeared and there exists a large gap between the fibres and the matrix. Because of the existence of this large gap, further oxidation of the carbon coating material could happen rapidly, and the coating may be completely oxidized throughout the composite [31]. The removal of the carbon interphase may change the interfacial shear strength, leading to the observed decrease in matrix cracking stress [14]. The oxidation of the carbon interphase may also affect the load transfer mechanism between the matrix and fibre and even damage the fibre itself [32] which will degrade the ultimate strength of the composite. It has been shown that the oxidation of the carbon coating in fibre-reinforced CVI SiC matrix composites can decrease both the matrix cracking stress and the ultimate strength [33].

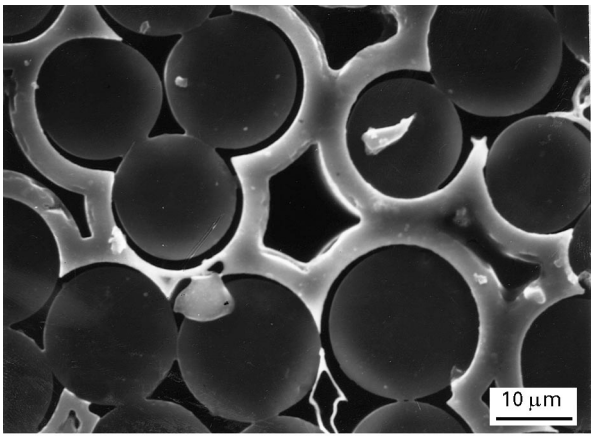

Figure 14 SEM micrograph showing the microstructure of the unidirectional composite quenched at $\Delta T = 1000\,^{\circ}\mathrm{C}$.

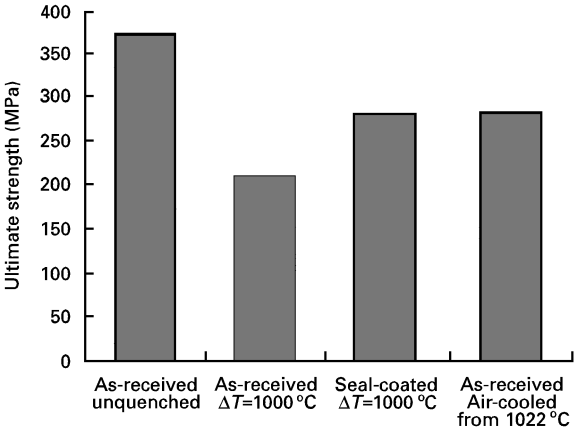

Figure 15 Effects of oxidation and thermal shock on the ultimate strength of the unidirectional composite.

Therefore, concern arose as to whether the property change we observed was caused by the thermal shock or oxidation. Some preliminary experiments were conducted in order to isolate the factors. The specimens prepared for the thermal shock test were sent to Oak Ridge National Laboratory where a SiC seal coating of ~ 40 μm thickness was applied by chemical vapour deposition. Fig. 15 shows the retained ultimate strengths of four specimens: (1) as-fabricated and unquenched, (2) as-fabricated and water quenched at $\Delta T = 1000\,^{\circ}\mathrm{C}$, (3) as-fabricated and air-cooled from 1022 °C, and (4) seal-coated and water quenched at $\Delta T = 1000\,^{\circ}\mathrm{C}$. It is seen that both specimens 3 and 4 show a decrease in the ultimate strength compared to the unquenched sample, while the as-fabricated and quenched specimen (specimen 2) exhibits the largest strength decrease, which indicates that both oxidation and water-quench can result in strength degradation individually, but the property change we saw in the present study was caused by the combined effects of oxidation and thermal shock.

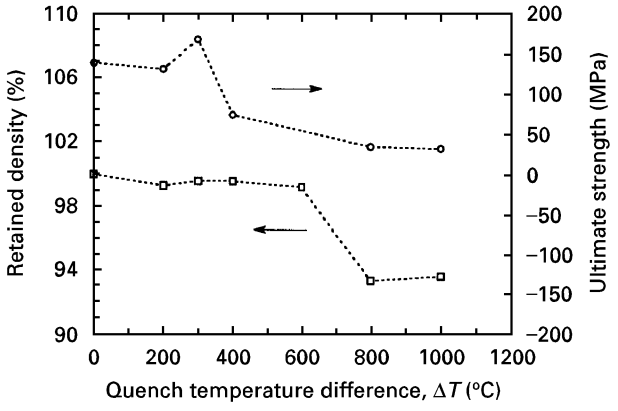

Figure 16 Effect of quench temperature difference on the density and ultimate strength of the 0°/90° composite.

In order to determine whether the critical temperature difference was also affected by the oxidation, the density change of the specimens quenched at different ΔT values was monitored. The result for the 0°/90° composite is plotted in Fig. 16 along with the ultimate strength as a function of ΔT. It is seen that the density of the composite starts to decrease as a result of the carbon oxidation at about 600 °C, much higher than the ΔT_c for the onset of the ultimate strength decrease (350 °C). Therefore, it is concluded that the ultimate strength decrease at the critical ΔT is caused solely by the thermal shock damage.

A detailed study is in progress to investigate the combined effects of the thermal shock and oxidation, which is of great practical significance because fibre-reinforced ceramic composites are often used under both thermal transients and oxidizing environments. Thermal shock induced microcracks in the matrix may accelerate the oxidation of the interphase and fibres, leading to enhanced degradation of composite properties, and oxidation may in turn change the thermal shock resistance of composites in service. In addition, a finite element modelling is being performed to determine the thermomechanical stresses developed during thermal shock tests and relate them to the experimental observations of this study.

5. Conclusions

The thermal shock behaviour of Nicalon™ fibre-reinforced CVI SiC matrix composites with three different types of fibre architecture: unidirectional, 0°/90°, and 2-D woven, has been studied using the water quench technique. Thermal shock induced damage was characterized by a destructive technique of four-point flexure and the nondestructive technique of Young's modulus measurement by the dynamic resonance method.

It has been shown that the composite with a 2-D fibre architecture possessed a superior resistance to thermal shock over the unidirectional and 0°/90° composites. The critical quench temperature difference for the onset of property degradation was higher for the 2-D composite, the property degradation was not catastrophic and at the maximum ΔT of 1000 °C, the 2-D composite was able to retain a significant portion of its original properties, including matrix cracking stress, ultimate strength, work of fracture, and Young's modulus. The poor mechanical properties and resistance to thermal shock of the unidirectional and 0°/90° composites were attributed to their low shear strengths and poor microstructures created during the carbon interfacial coating and CVI processing. Excess carbon interfacial coating material was present in the unidirectional and 0°/90° composites, which blocked the uniform infiltration of SiC around the fibres. In addition, the anisotropy of the unidirectional and 0°/90° fibre architectures prevented the composites from attaining high density during infiltration. By contrast, the composite with a 2-D woven fibre architecture and 0°/30°/60° cloth lay-up showed superior mechanical properties and thermal shock resistance. Oxidation of the carbon coating was found to contribute to the property degradation at high quench temperature difference. However, the onset of the gradual decrease in matrix cracking stress and ultimate strength was caused by the thermal shock.

The nondestructive technique of Young's modulus measurement by the dynamic resonance method successfully detected the damage by thermal shock. The critical quench temperature differences for the onset of the property degradation determined by the NDE technique either coincided with or were lower than those by the destructive technique, which indicated the feasibility and possibly higher sensitivity of the NDE technique.

Acknowledgements

This research is sponsored by the U.S. Department of Energy, Assistant Secretary for Energy Efficiency and Renewable Energy, Office of Industrial Technologies, Industrial Energy Efficiency Division and CFCCs Program, under contract DE-AC05-84OR21400 managed by Martin Marietta Energy Systems, Inc.

References

1. H. WANG, R. N. SINGH and R. A. LOWDEN, *J. Amer. Ceram. Soc.* **79** (1996) 1783.
2. H. WANG and R. N. SINGH, *Int. Mater. Reviews* **39** (1994) 228.
3. *Idem.*, *Ceram. Engng. Sci. Proc.* **15** (1994) 292.
4. D. BELITSKUS, in "Fibre and Whisker Reinforced Ceramics for Structural Applications" (Marcel Dekker, New York, 1993) Ch. 6.
5. C. H. WEBER, J. P. A. LOFVANDER and A. G. EVANS, *J. Amer. Ceram. Soc.* **77** (1994) 1745.
6. H. H. K. XU, C. P. OSTERTAG and L. M. BRAUN, *ibid.* **77** (1994) 1889.
7. *Idem.*, *ibid.* **77** (1994) 1897.
8. D. S. BEYERLE, S. M. SPEARING, F. W. ZOK and A. G. EVANS, *ibid.* **75** (1992) 2719.
9. J. LLORCA and R. N. SINGH, *ibid.* **74** (1991) 2882.
10. R. N. SINGH, *ibid.* **73** (1990) 2930.
11. *Idem.*, *ibid.* **73** (1990) 2399.
12. A. G. EVANS, *Mater. Sci. Engng.* **A107** (1989) 227.
13. D. B. MARSHALL and A. G. EVANS, *J. Amer. Ceram. Soc.* **68** (1985) 225.
14. D. B. MARSHALL, B. N. COX and A. G. EVANS, *Acta Metall.* **33** (1985) 2013.

15. D. S. BEYERLE, S. M. SPEARING and A. G. EVANS, *J. Amer. Ceram. Soc.* **75** (1992) 3321.
16. O. SBAIZERO and A. G. EVANS, *ibid.* **69** (1986) 481.
17. P. BRONDSTED, F. E. HEREDIA and A. G. EVANS, *ibid.* **77** (1994) 481.
18. X. AUBARD and J. LAMON, *ibid.* **77** (1994) 2118.
19. R. A. NAIK, P. G. IFJU and J. E. MASTERS, *J. Comp. Mater.* **28** (1994) 656.
20. P. F. TORTORELLI, C. A. WIJAYAWARDHANA, L. RIESTER and R. A. LOWDEN, *Ceram. Engng. Sci. Proc.* **15** (1994) 262.
21. K. R. VAIDYANATHAN, J. SANKAR, A. D. KELKAR and J. NARAYAN, *ibid.* **15** (1994) 281.
22. J. P. SINGH, D. SINGH and R. A. LOWDEN, *ibid.* **15** (1994) 456.
23. S. PROUHET, G. CAMUS, C. LABRUGERE, A. GUETTE and E. MARTIN, *J. Amer. Ceram. Soc.* **77** (1994) 649.
24. N. CHAWLA, P. K. LIAW, E. LARA-CURZIO, R. A. LOWDEN and M. K. FERBER, in "High performance composites: commonalty of phenomena", edited by K. K. Chawla and S. G. Fishman (The Minerals, Metals & Materials Society, Warrandale, PA, 1994) pp. 291–304.
25. B. L. WEAVER, R. A. LOWDEN, J. C. MCLAUGHLIN, D. P. STINTON, T. M. BESMAN and O. J. SCHWARZ, *Ceram. Engng. Sci. Proc.* **14** (1993) 1008.
26. A. S. FAREED, B. SONUPARLAK, C. T. LEE, A. J. FORTINI and G. H. SCHIROKY, *ibid.* **11** (1990) 782.
27. D. P. STINTON, A. J. CAPUTO and R. A. LOWDEN, *Amer. Ceram. Soc. Bull.* **65** (1986) 347.
28. P. J. LAMICQ, G. A. BERNHART, M. M. DAUCHIER and J. G. MACE, *ibid.* **65** (1986) 336.
29. E. FITZER and R. GADOW, *ibid.* **65** (1986) 326.
30. S. P. TIMOSHENKO and J. M. GERE, in "Mechanics of Materials" (Van Nostrand Reinhold, New York, 1972) Ch. 5.
31. K. L. LUTHRA, *Ceram. Tran.* **10** (1990) 183.
32. T.-I. MAH, M. G. MENDIRATTA, A. P. KATZ and K. S. MAZDIYASNI, *Ceram. Bull.* **66** (1987) 304.
33. P. F. TORTORELLI, S. NIJHAWAN, L. RIESTER and R. A. LOWDEN, *ibid.* **14** (1993) 358.

Received 10 August 1995
and accepted 21 October 1996